Applied Mathematical Sciences, Vol. 12, 2018, no. 1, 37 - 45
HIKARI Ltd, www.m-hikari.com
https://doi.org/10.12988/ams.2018.712360

Mathematical Modeling of Solid Oxide Fuel Cell Fed Biomass Derived Fuel

Sineenart Srimongkol

Department of Mathematics, Faculty of Science
Burapha University, Thailand
Centre of Excellence in Mathematics
PERDO, CHE, Thailand

Abstract

Biomass derived fuel has been widely used in Thailand. The solid oxide fuel cell can fed variety of fuels. Moreover, the experimental cost of the solid oxide fuel cell is very expensive. Therefore, the mathematical model of solid oxide fuel with biomass derived fuel is crucial. The governing equations for solid oxide fuel are the fully coupled of the current balance equations, the mass transport equations, and the Brinkman equations. Taken into account the biomass derived fuel, the chemical reactions from the gasifying process reveal that the hydrogen mole fraction is controlled. The effect of the hydrogen mole fraction is investigate. The results indicate that increase the mass fraction, the average current density is not increase. The electrolyte current density with high initial hydrogen mass fraction has the good distribution at the center of the solid oxide fuel cell than the lower one.

Mathematics Subject Classification: 93A30

Keywords: Solid oxide fuel cell, Mathematical model, Biofuel, Biomass derived fuel

1 Introduction

Due to the energy problem, the renewable energy such as wind power, solar energy, nuclear energy, biofuel including hydrogen energy is a possible solu-

tion [4, 9]. Fuel cell is a device using hydrogen for the electrical power. It was firstly developed in 1983 by Friderich Schnbein. Nowadays, the fuel cells research works are focused on the development of various fuel cell for powers and transportation. Fuel cell can be classified as alkaline fuel cell (AFC), phosphoric acid fuel cell (PAFC), molten carbonate fuel cell (MCFC), polymer electrolyte membrane fuel cell (PEMFC), direct methanol fuel cell (DMFC), and solid oxide fuel cell (SOFC) [5, 7, 13]. Solid oxide fuel cell has the high efficiency (50-60%), high operating temperature (650-1,000 $^{\circ}C$) and flexibility of feeding fuels not only pure hydrogen, but also many reformate composition consisting of multi-component species maybe used as fuel, such as water (H_2O), carbonmonoxide (CO), carbondioxide (CO_2), including biofuel [2, 6, 10]. In Thailand, biofuel is developed due to the rich of resources [3, 8, 11, 14, 15].

The liquid biofuel or bio ethanol or bio-oil can produce purify hydrogen by steam-iron process [1, 12]. It is gasifying as following chemical reaction,

$$\mathrm{C_nH_mO_p} + (2\mathrm{n} - \mathrm{p})\mathrm{H_2O} + \mathrm{nCaO} \rightarrow \mathrm{nCaCO_3} + \left(\frac{\mathrm{m}}{2} - 2\mathrm{n} - \mathrm{p}\right)\mathrm{H_2}.$$

The syngas from the biomass gasifier enters the prereformer and CO is converted to H_2 and CO_2. In the pre-reformer CH_4 and CO are converted into the hydrogen using the steam agent. The chemical reactions are as follow,

$$\mathrm{CH_4} + \mathrm{H_2O} \rightarrow \mathrm{CO} + 3\mathrm{H_2},$$

$$\mathrm{CO} + \mathrm{H_2O} \rightarrow \mathrm{CO_2} + \mathrm{H_2},$$

$$\mathrm{CH_4} + 2\mathrm{H_2O} \rightarrow \mathrm{CO_2} + 4\mathrm{H_2}.$$

The chemical reactions in the solid oxide fuel cell system consist of the reaction in anode and cathode, respectively,

$$\mathrm{H_2} + \mathrm{O^{2-}} \rightarrow \mathrm{H_2O} + 2\mathrm{e^-},$$

$$\frac{1}{2}\mathrm{O_2} + 2\mathrm{e^-} \rightarrow \mathrm{O^{2-}}.$$

The overall reaction is

$$\frac{1}{2}\mathrm{O_2} + \mathrm{H_2} \rightarrow \mathrm{H_2O}.$$

The flow of the chemical reaction for producing the electrical current is shown in figure 1.

From the purified hydrogen process from liquid biofuel and syngas from biomass gasifier, the hydrogen is produced. The solid oxide fuel cell will obtain the rich hydrogen from those processes. However, how much hydrogen should increase the performance of the solid oxide fuel cell? Therefore, the effect of the hydrogen mass fraction is investigated.

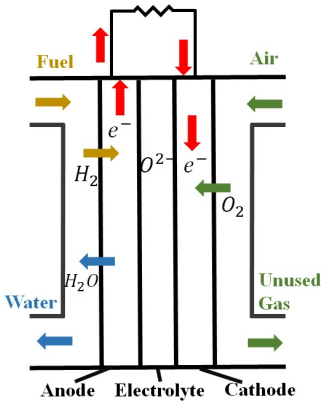

Figure 1: Solid oxide fuel cell and the flow of the chemical reaction to produce the electrical current.

2 Mathematical Model

Solid oxide fuel cells can produce more electrical power by increase the cells into the stack. Therefore, the performance of the solid oxide fuel cell is investigated using a single cell as shown in the figure 2 The computational domain is created

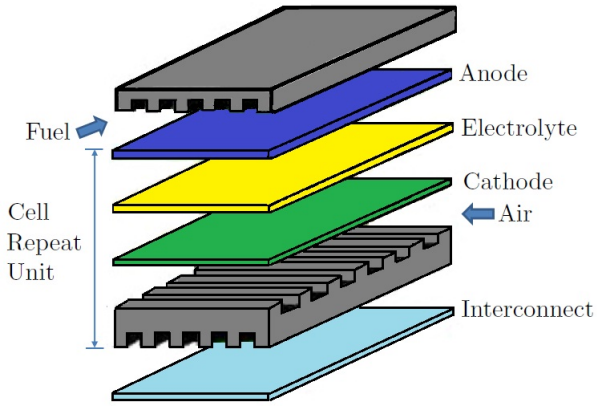

Figure 2: Three dimensional of a single cell planar solid oxide fuel cell.

as shown in the figure 3.

2.1 Governing Equations

The governing equations consist of Maxwell-Stefan equations as shown in equation (1)

$$\frac{\partial}{\partial t}\left(\rho \mathbf{c}_i\right) + \nabla \cdot \left(\rho \mathbf{c}_i \mathbf{u}\right) = -\nabla \cdot \mathbf{j}_i + \mathbf{R}_i \tag{1}$$

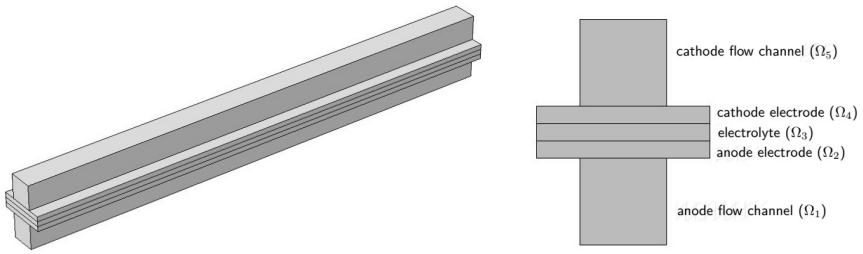

Figure 3: Configuration of a unit cell solid oxide fuel cell; anode flow channel (Ω_1), anode electrode (Ω_2), electrolyte (Ω_3), cathode electrode (Ω_4), and cathode flow channel (Ω_5).

where, ρ (kg/m^3) is the mixture density, $\mathbf{u}$ (m/s) is the mass average velocity of the mixture, c_i is the mass fraction, $\mathbf{j}_i$ $(kg/(m^2 s))$ is the mass flux relative to the mass average velocity, and R_i $(kg/(m^3 s))$ is the rate expression describing its production or consumption.

The current balance in the electrolyte is governed by

$$\nabla \cdot \mathbf{J} = \mathbf{Q}, \quad \text{in } \Omega_2,\, \Omega_3,\, \Omega_4 \tag{2}$$

where $\mathbf{J}$ denotes the current density vector in the electrolyte, $\mathbf{Q}$ can be any source or sink. Navier-Stokes equations for describing the flow in open regions, and the Brinkman equations for the flow in porous regions.

$$\frac{\partial \rho}{\partial t} + \nabla \cdot (\rho \mathbf{u_c}) = 0, \tag{3}$$

$$\rho \frac{\partial \mathbf{u_c}}{\partial t} + \rho \left(\mathbf{u_c} \cdot \nabla\right) \mathbf{u_c} = \nabla \cdot \left[-pc\mathbf{I} + \mu \left(\nabla \mathbf{u_c} + (\nabla \mathbf{u_c})^T \right) - \frac{2}{3}\mu \left(\nabla \cdot \mathbf{u_c}\right) \mathbf{I} \right] + \mathbf{F}, \tag{4}$$

$$\frac{\partial \left(\epsilon_p \rho\right)}{\partial t} + \nabla \cdot (\rho \mathbf{u_c}) = Q_{br} \tag{5}$$

$$\frac{\rho}{\epsilon_p} \left(\frac{\partial \mathbf{u_c}}{\partial t} + \left(\mathbf{u_c} \cdot \nabla\right) \frac{\mathbf{u_c}}{\epsilon_p} \right) \tag{6}$$

$$= \nabla \cdot \left[-pc\mathbf{I} + \frac{\mu}{\epsilon_p} \left(\nabla \mathbf{u_c} + (\nabla \mathbf{u_c})^T \right) - \frac{2\mu}{3\epsilon_p} \left(\nabla \cdot \mathbf{u_c}\right) \mathbf{I} \right] \tag{7}$$

$$- \left(\frac{\mu}{\kappa_{br}} + \beta_F |\mathbf{u_c}| + \frac{Q_{br}}{\epsilon_p^2} \right) \mathbf{u_c} + F \tag{8}$$

where μ $(kg/(m \cdot s))$ is the dynamic viscosity, $\mathbf{uc}$ (m/s) is the velocity vector, ρ (kg/m^3) is the density, pc (Pa) is the pressure, ϵ_p is the porosity, κ_p (m^2) is the permeability of the porous medium, and Q_{br} $(kg/(m^3 \cdot s))$ is a mass source or sink. $\beta_F |\mathbf{u_c}| \mathbf{u_c}$ is viscous force proportional to the square of the fluid velocity where β_F is the Forchheimer drag option (kg/m^4).

2.2 Boundary Conditions

The fuel feed in the cathode and anode is counterflow, with hydrogen-rich anode gas entering from the left. For the ionic charge balance equations in cathode electrode, electrolyte, and anode electrode, the insulating boundary condition is applied on all external boundaries as shown below.

$$-\mathbf{n} \cdot \mathbf{J} = 0. \tag{9}$$

For the transport of species in anode, initial mass fraction (ω_{h_2}) 0.04, and 0.2 are used at the left of the anode flow channel. The outflow is at the right of the anode flow channel. No flux boundary condition is applied to all external boundaries of the anode electrode and the anode flow channel as given below.

$$-\mathbf{n} \cdot (\mathbf{j}_i + \rho \mathbf{u} \omega_i) = 0. \tag{10}$$

3 Numerical Simulation

The computational mesh is consisted of 9,744 hexahedral elements as shown in figure 4. The numerical solutions of the fully couple equations (1) - (8) and all boundary conditions are obtained by Comsol Multiphysics 5.2.

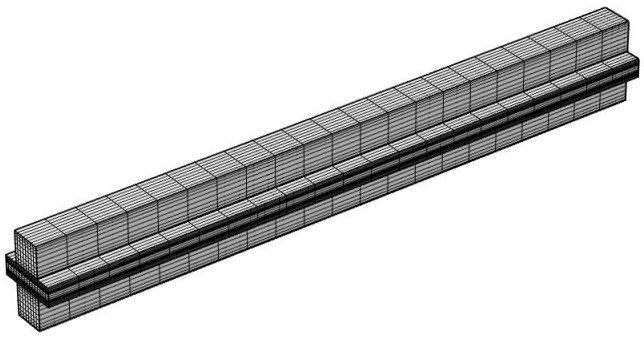

Figure 4: Computational mesh for a unit cell solid oxide fuel cell consists of 9,744 elements.

To investigate the effect of hydrogen mole fraction to the performance of solid oxide fuel cell, the hydrogen mole fraction 0.04, and 0.2 are used in the initial values. The plots of the distribution of the hydrogen mole fraction in the anode electrode and anode flow channel with the initial hydrogen mole fraction 0.04, and 0.2, respectively, are shown in figure 5. The highest value of the hydrogen mole fraction is at the inlet and gradually decrease with quite

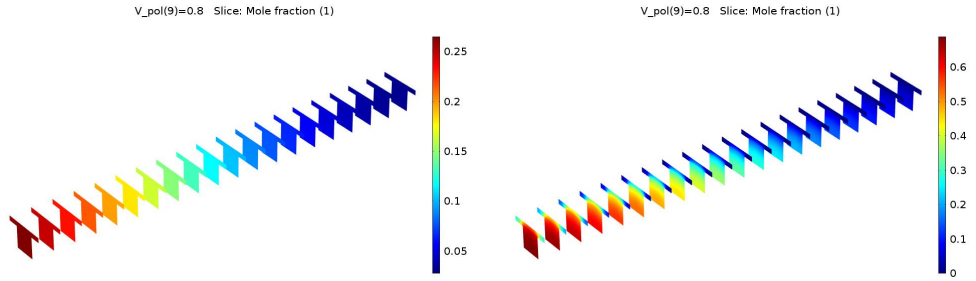

Figure 5: Hydrogen mole fraction with the initial mass fraction $\omega_{h_2} = 0.04, 0.2$, respectively

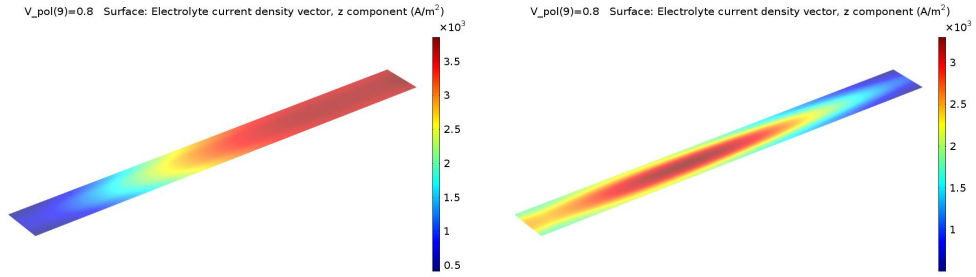

Figure 6: Electrolyte current density with the initial mass fraction $\omega_{h_2} = 0.04, 0.2$, respectively

same pattern for both initial values. Figure 6 is the plots of the electrolyte current density in the center of the solid oxide fuel cell with the the initial hydrogen mole fraction 0.04, and 0.2, respectively. The high current density is located at the end of the solid oxide fuel cell for the initial hydrogen mole fraction 0.04 while the high current density is located at the center of the solid oxide fuel cell for the initial hydrogen mole fraction 0.2. The polarization curves of the solid oxide fuel cell with the initial hydrogen mole fraction 0.04, and 0.2, respectively, are shown in figure 7. The initial mas fraction 0.04, the maximum average current density is around 2,700 A/m^2 which is more than other around 500 A/m^2.

4 Conclusion and Discussion

The variety of fuels can used for feeding solid oxide fuel cell. The biofuel of biogas are the government support fuel in Thailand. In this research, the effect of the hydrogen mass fraction is investigated when the biofuel and biogas are changed to hydrogen due to the chemical reactions. A mathematical model of solid oxide fuel cell is fully coupled the mass transport equations, the Maxwell-Stefan Equations, the Navier-Stoke Equations and the Brinkman

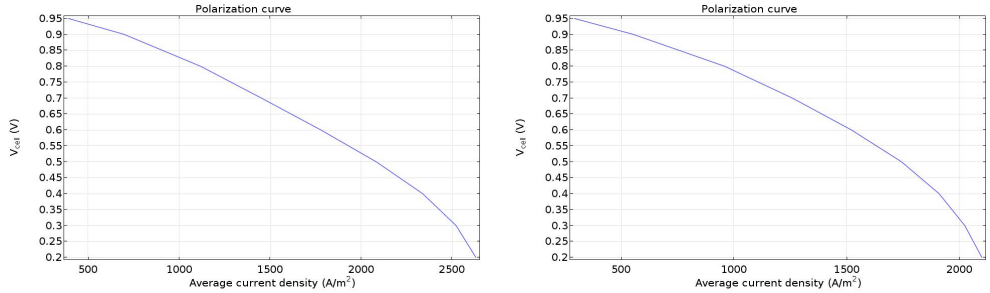

Figure 7: Polarization curve with the initial mass fraction $\omega_{h_2} = 0.04, 0.2$, respectively

equations with the appropriate boundary conditions. The governing equations and boundary conditions are solved using Comsol Multiphysic 5.2. The results indicate that increase the mass fraction, the average current density as shown in polarization graph is not increase. The electrolyte current density with hydrogen initial mass fraction 0.2 has the good distribution at the center of the solid oxide fuel cell. However, the initial mass fraction of hydrogen is used only 2 values. To improve the results more values of the hydrogen mole fraction have to taken into account to find the relation between hydrogen mass fraction with the performance of the solid oxide fuel.

Acknowledgements. This work was financially supported by the Research Grant of Burapha University through National Research Council of Thailand (Grant no.21/2560).

References

[1] M. Aghie, M. Mehrpooya and F. Pourfayaz, Introducing an integrated chemical looping hydrogen production, inherent carbon capture and solid oxide fuel cell biomass fueled power plant process configuration, *Energy Conversion and Management*, **124** (2016), 141 - 154. https://doi.org/10.1016/j.enconman.2016.07.001

[2] L.E. Arteaga-Prez, Y. Casas-Ledon, R. Perez-Bermudez, L.M. Peralta, J. Dewulf and W. Prins, Energy and exergy analysis of a sugar cane bagasse gasifier integrated to a solid oxide fuel cell based on a quasi-equilibrium approach, *Chemical Engineering Journal*, **228** (2013), 1121 - 1132. https://doi.org/10.1016/j.cej.2013.05.077

[3] D.R. Bell, T. Silalertruksa, S.H. Gheewala and R. Kamens, The net cost of biofuels in Thailand: an economic analysis, *Energy Policy*, **39** (2011), 834 - 843. https://doi.org/10.1016/j.enpol.2010.11.002

[4] W. Cai, Q. Zhou, Y. Xie, J. Liu, G. Long, S. Cheng and M. Liu, A direct carbon solid oxide fuel cell operated on a plant derived biofuel with natural catalyst, *Applied Energy*, **179** (2016), 1232 - 1241. https://doi.org/10.1016/j.apenergy.2016.07.068

[5] S.A. Hajimolana, M. Azlan Hussain, W.M.A. Wan, M. Soroush and A. Shamiri, Mathematical modeling of solid oxide fuel cells: A review, *Renewable and Sustainable Energy Reviews*, **15** (2011), 1893 - 1917. https://doi.org/10.1016/j.rser.2010.12.011

[6] W.T. Hong, T.H. Yen, T.D. Chung, C.N. Huang and B.D. Chen, Efficiency analyses of ethanol-fueled solid oxide fuel cell power system, *Applied Energy*, **88** (2011), 3990 - 3998. https://doi.org/10.1016/j.apenergy.2011.03.044

[7] S. Kakac, A. Pramuanjaroenkij and X.Y. Zhou, A review of numerical modeling of solid oxide fuel cells, *International Journal of Hydrogen Energy*, **32** (2007), 761 - 786. https://doi.org/10.1016/j.ijhydene.2006.11.028

[8] N. Lecksiwilai, S.H. Gheewala, T. Silalertruksa and J. Mungkalasiri, LCA of biofuels in Thailand using thai ecological scarcity method, *Journal of Cleaner Production*, **142** (2017), 1183 - 1191. https://doi.org/10.1016/j.jclepro.2016.07.054

[9] J. Lin, T.A. Trabold, M.R. Walluk and D.F. Smith, Bio-fuel reforming for solid oxide fuel cell applications. Part 2: Biodiesel, *International Journal of Hydrogen Energy* **39** (2014), 183 - 195. https://doi.org/10.1016/j.ijhydene.2013.10.058

[10] S. Liu, W. Kong, and Z. Lin, Three-dimensional modeling of planar solid oxide fuel cells and the rib design optimization, *Journal of Power Sources*, **194** (2009), 854 - 863. https://doi.org/10.1016/j.jpowsour.2009.06.056

[11] P. Nimmanterdwong, B. Chalermsinsuwan and P. Piumsomboon, Emergy evaluation of biofuels production in Thailand from different feedstocks, *Ecological Engineering*, **74** (2015), 423 - 437. https://doi.org/10.1016/j.ecoleng.2014.11.017

[12] J. Plou, P. Duran, J. Herguido and J.A. Pena, Hydrogen from bio-fuels by "steam-iron" process: Modelling and kinetics, *International Journal of Hydrogen Energy*, **41** (2016), 19349 - 19356. https://doi.org/10.1016/j.ijhydene.2016.05.127

[13] K. Sadik, P.J.B. Anchasa, and X.Y. Zhou, A review of numerical modeling of solid oxide fuel cells, *International Journal of Hydrogen Energy*, **32** (2007), 761 - 786. https://doi.org/10.1016/j.ijhydene.2006.11.028

[14] S. Wianwiwat and J. Asafu-Adjaye, Is there a role for biofuels in promoting energy self sufficiency and security? A CGE analysis of biofuel policy in Thailand, *Energy Policy*, **55** (2013), 543 - 555.
https://doi.org/10.1016/j.enpol.2012.12.054

[15] J. Xuan, M.K.H. Leung, D.Y.C. Leung and M. Ni, A review of biomass-derived fuel processors for fuel cell systems, *Renewable and Sustanable Energy Reviews,* **13** (2009), 1301 - 1313.
https://doi.org/10.1016/j.rser.2008.09.027

Received: December 27, 2017; Published: January 10, 2018